Received: 23 January 2025 | Accepted: 15 August 2025

DOI: 10.1111/1365-2435.70158

BRITISH ECOLOGICAL SOCIETY Functional Ecology

RESEARCH ARTICLE

The spatial scaling of multiple dimensions of functional diversity in habitat islands

Rafael Antunes Dias[1] | **Vinicius Augusto Galvão Bastazini**[2] | **Andros T. Gianuca**[3] | **Thomas J. Matthews**[4,5]

[1]Laboratório de Ecologia de Mamíferos e Aves, Universidade Federal de Pelotas, Pelotas, Brazil

[2]Independent Researcher, Nivelles, Belgium

[3]PPG Ecologia, Universidade Federal do Rio Grande do Norte, Natal, Brazil

[4]School of Geography, Earth and Environmental Sciences (GEES) and Birmingham Institute of Forest Research, University of Birmingham, Birmingham, UK

[5]CE3C – Centre for Ecology, Evolution and Environmental Changes/Azorean Biodiversity Group and Universidade dos Açores – Depto de Ciências Agráriase Engenharia do Ambiente, Angra do Heroísmo, Açores, Portugal

Correspondence
Rafael Antunes Dias
Email: rafael.dias@ufpel.edu.br

Handling Editor: Qiang Yang

Abstract

1. Functional diversity is a multidimensional concept, with different dimensions capturing how functional traits are distributed within communities. Exploring how these dimensions scale with island area (functional diversity–area relationships [FDARs]) is key to understanding how habitat size shapes diversity and community assembly.
2. Using avian abundance and richness data from three habitat-island systems in southern Brazil, we analysed FDARs using three dimensions - functional richness (FRic), divergence (FDiv) and regularity (FReg) - to test how species abundance influences FDAR form, how FDARs differ among dimensions, and how standardized functional diversity values scale with island area.
3. FDARs were modelled using a multimodel approach to assess their form, while null models were used to obtain standardised effect sizes (SES) of all indices.
4. Abundance had little influence on FDAR form due to strong correlations with species richness. FRic increased more steeply with area than FDiv, while FReg declined, revealing distinct scaling patterns and showing that habitat loss affects FD dimensions differently. SES showed no relationship with area, underscoring that species richness is the main driver of FDARs in these habitat island systems.
5. Community assembly seemed to be largely driven by neutral dynamics, with only a relatively small number of islands characterised by trait clustering and little evidence of overdispersion. However, the prevalence of non-random assembly patterns varied with island size and across habitat island systems and functional diversity dimensions, the latter finding suggesting that different dimensions may capture distinct assembly processes.
6. These findings underscore the importance of using multidimensional functional diversity approaches to disentangle complex assembly processes and guide conservation strategies in patchy ecosystems.

KEYWORDS
community assembly patterns, functional divergence, functional regularity, functional richness, kernel density *n*-dimensional hypervolumes

---

1 | INTRODUCTION

Assessing the spatial scaling of diversity is essential if we are to understand how habitat area and habitat loss affect ecological systems. This is often approached through the study of species–area relationships, which model how species richness is related to area (Lomolino, 2000; Matthews & Rigal, 2021). However, diversity extends beyond species richness, the basis of traditional species–area relationships, to include a functional facet (Cadotte et al., 2013; Mazel & Thuiller, 2021). The alpha diversity (FDα) of this functional facet can be assessed through measuring three complementary dimensions: functional richness (FRic), the sum of trait differences among taxa; functional divergence (FDiv), the average difference between taxa; and functional regularity (FReg, sometimes called 'functional evenness'), how regular the differences between taxa are (the 'Pavoine–Bonsall' scheme; Mammola et al., 2021; Pavoine & Bonsall, 2011). Due to the complementary nature of diversity facets, evaluating area effects beyond species richness within a unified analytical framework is essential if we are to develop a mechanistic understanding of biodiversity patterns and ecosystem functioning (Mazel & Thuiller, 2021).

Island functional diversity–area relationships (FDARs) describe how some measure of functional diversity scales with island area (Mazel & Thuiller, 2021; Smith et al., 2013). Since functional traits mediate interactions between organisms and their environment, these relationships assist in revealing how spatial processes influence community structure, assembly and ecosystem functioning on islands (Matthews et al., 2023; Mazel & Thuiller, 2021). A common approach in FDAR studies is to assess the shape and slope of the relationship using data from multiple island systems (Matthews, 2021; Matthews et al., 2023). Different model shapes and slopes carry distinct theoretical and practical implications, underscoring the relevance of this approach for informing conservation strategies (Matthews et al., 2023). For example, convex and asymptotic curves may emphasize the conservation value of small patches by reflecting rapid trait accumulation with area across small habitat islands and, in the case of the latter, eventual saturation in FDα with increasing area, while sigmoidal and non-saturating curves reveal thresholds or non-asymptotic increases in FDα with area that highlight the relatively greater importance of larger habitat patches (Matthews et al., 2023; Mazel & Thuiller, 2021).

Traditionally, FDARs have been explored using the richness dimension of FDα, with FRic typically best fitted by convex or sigmoidal, upward-oriented, non-asymptotic models from the power and exponential families (Dias et al., 2020; Gao & Wang, 2024; Karadimou et al., 2016; Matthews et al., 2023; Mazel & Thuiller, 2021). Work to date has shown that FRic FDARs are largely driven by species richness, since controlling for the effect of richness leads to weak, flat or downward-oriented relationships (Dias et al., 2020; Gao & Wang, 2024; Matthews et al., 2023). Comparative studies have also shown that species richness tends to accumulate faster with area than FRic (Dias et al., 2020; Matthews et al., 2023). Despite such advances, key gaps remain in our understanding of FRic FDARs. For example, the impact of species abundance on FRic FDARs is unknown due to data and methodological limitations. Species abundance patterns influence species–area relationships (Chase et al., 2019; Tjørve et al., 2008) and likely affect FRic–area patterns as well, but exactly how abundance shapes the form of abundance-weighted FRic FDARs remains unknown.

In contrast to FRic, the scaling of other FDα dimensions with area has received comparatively less attention. FDiv tends to show highly idiosyncratic patterns, while FReg has been shown to decline with area, suggesting less even trait distributions in larger habitats (Ding et al., 2013; Ferrari et al., 2023; Gao & Wang, 2024; Karadimou et al., 2016). Yet, the extent to which these trends hold across spatial scales remains unclear (Karadimou et al., 2016). How FDiv and FReg scale with area, once any effect of species richness on these indices is controlled for, also remains poorly understood (Ding et al., 2013; Ferrari et al., 2023; Mouchet et al., 2010).

Studies assessing how FDα scales with area independently of species richness have usually employed null models to derive standardized effect sizes (SES; Dias et al., 2020; Gao & Wang, 2024; Matthews et al., 2023). FDα.SES values are of additional importance as they provide insight into island trait-based community assembly, with negative SES values indicating trait clustering and positive values indicating trait overdispersion (Mazel & Thuiller, 2021). Clustering is typically seen as being indicative of the process of environmental filtering, whereby specific trait values are sampled from the species pool (i.e. species are functionally more similar than expected by chance in local communities; Mazel & Thuiller, 2021; Weiher & Keddy, 1995). Interspecific competition, which is expected to promote resource partitioning among species, is predicted to result in a pattern of trait overdispersion (i.e. species being functionally less similar than expected by chance in local communities) if traits stabilize niche differences, or a pattern of trait clustering if traits equalize fitness differences (Mayfield & Levine, 2010; Mazel & Thuiller, 2021; Weiher & Keddy, 1995). While some previous studies using FRic.SES have shown that trait-based community assembly on islands is largely shaped by random processes (Dias et al., 2020; Gao & Wang, 2024; Matthews et al., 2023), we still lack a general understanding of how assembly patterns (i.e. clustering, overdispersion, random) scale with island area, particularly in habitat islands.

Here, we combined high-resolution data on avian functional traits with kernel density *n*-dimensional hypervolumes to generate FDα indices measuring the richness, divergence and regularity dimensions of FDα, and model avian FDARs in three habitat island systems with varying species pool sizes, matrix contrasts and habitat diversity (Dias et al., 2020). Habitat islands are defined as isolates surrounded by non-aquatic and relatively permeable matrix habitats that allow some island species to colonize the matrix and vice versa (Matthews, 2021). Due to their mobility, habitat dependence and the availability of detailed data on their functional traits, birds are ideal model organisms for investigating how habitat island area influences functional diversity and associated community assembly patterns (Dias et al., 2020; Matthews et al., 2023; Tobias et al., 2022). The use of *n*-dimensional hypervolumes enabled us to employ a unified analytical framework that allows for the calculation of multidimensional measures of FDα (FRic, FDiv and FReg) while also incorporating abundance data (Mammola et al., 2021; Mammola & Cardoso, 2020; Palacio et al., 2022). We addressed three primary knowledge gaps in FDAR research: (i) How does the inclusion of abundance data affect the form of FRic–area relationships; (ii) what are the similarities and differences between FDARs calculated using different FDα dimensions; and (iii) how standardized FD values (i.e. FDα.SES values) scale with habitat island area and how different trait-based community assembly patterns are distributed across the area gradient.

1.1 | Theoretical expectations

1.1.1 | Knowledge gap I

We expect that the form of abundance-weighted FRic FDARs would resemble presence–absence FRic FDARs, both being characterized as positive convex-upward relationships, due to the correlations between FRic, species richness and abundance (Ding et al., 2013; Ferrari et al., 2023; Gao & Wang, 2024; Karadimou et al., 2016). We focussed solely on FRic to address this knowledge gap because existing analyses of FDiv and FReg already commonly incorporate abundance data (Mammola et al., 2021; Mammola & Cardoso, 2020).

1.1.2 | Knowledge gap II

FDiv is expected to increase with area, as larger habitat islands facilitate the coexistence of many functionally distinct abundant species, either across the entire functional space or in dispersed clusters, owing to increased niche space (Mouchet et al., 2010; Villéger et al., 2008). FReg, on the other hand, is expected to negatively correlate with area. In smaller areas, where interspecific competition may be more intense, the few species present are expected to exhibit trait differentiation that reduces resource use overlap and results in more even spacing of species in trait space, increasing FReg (Ding et al., 2013; Ferrari et al., 2023; Karadimou et al., 2016). In larger areas, FReg is expected to decline if certain trait combinations become overrepresented due to increased abundance or redundancy effects, leading to uneven distributions of species and individuals in trait space despite increased species richness (Ding et al., 2013; Ferrari et al., 2023; Karadimou et al., 2016). We predict that there will be an initial rapid increase in FDiv with area, followed by a slowing rate for larger habitat islands, and thus that FDiv FDARs will be best fitted by convex, non-asymptotic models, mirroring FRic FDARs (Ding et al., 2013; Gao & Wang, 2024; Karadimou et al., 2016). The same is expected for FReg FDARs, except that the relationship is predicted to be negative.

1.1.3 | Knowledge gap III

We expect that correcting for the effect of species richness on FDα indices will yield flat FDARs, as strong relationships between raw FDα values and area typically arise from correlations between functional and taxonomic diversity (Dias et al., 2020; Matthews et al., 2023). Habitat islands are typically 'noisy' and relatively disturbed systems where communities are predicted to assemble primarily through neutral dynamics (Dias et al., 2020; MacArthur & Wilson, 1967; Matthews, 2021; Matthews et al., 2023). Given this, and the results of previous studies (Dias et al., 2020; Matthews et al., 2023), we expect that most islands in our dataset will exhibit random community assembly patterns, with no systematic relationship between FDα.SES values and island size.

2 | MATERIALS AND METHODS

2.1 | Habitat islands

Our data comprise three independent, natural small-scale habitat island systems in Brazil (images of habitat-islands and additional details on the sites are available in Dias et al., 2020): (i) wet grassland patches in swales and depressions surrounded by drier grasslands ($n=46$ habitat islands; min–max area = 0.003–0.160 km^2; total area sampled = 1.696 km^2; extent of the landscape where sampling was conducted = 5297.69 km^2); (ii) bulrush patches in flooded, low-lying herbaceous vegetation ($n=42$; 0.0001–0.0708; 0.3024 km^2; 19.05 km^2); and (iii) washouts on a sandy marine beach ($n=22$; 0.0003–0.0432 km^2; 0.1158 km^2; ca. 70 km stretch). The limits of the habitat islands were marked in the field using a handheld GPS (±5 m error). These data were uploaded to Google Earth where the area was calculated in km^2. Our sample of habitat islands represents the range of their variability in the landscape. The grassland system has a larger spatial extent, larger habitat islands, higher habitat heterogeneity and a more permeable matrix (Dias et al., 2020). The bulrush and washout systems are smaller and more homogeneous, with the former displaying a high contrast with the matrix (Dias et al., 2020).

2.2 | Replication statement

Scale of inference	Scale at which the factor of interest is applied	Number of replicates at the appropriate scale
Habitat island systems in the landscape	Individual habitat islands	46, 42 and 22 habitat islands in three habitat island systems

2.3 | Bird sampling

Bird counts were carried out at dawn and dusk when birds are more detectable (Dias et al., 2020). Each island was surveyed once by two observers walking its full length along the longest axis. The survey covered all points located 10 m inside the perimeter of the island. All birds seen or heard on each sampled island were counted. We used low-volume playback to enhance detection of a few elusive species strictly associated with island habitats, while minimizing the risk of attracting individuals from neighbouring islands. Although we acknowledge that the small size of some habitat islands may allow for transient or partially resident individuals to be counted, most bird species detected, even on the smallest islands, were residents adapted to habitat conditions that differed markedly from the surrounding matrix (Dias et al., 2020). In grassland and bulrush islands, surveys were conducted during the breeding season to further minimize the likelihood of detecting transient individuals. Species richness (SR) is higher in grasslands, with a range of 3–45 species per island and a total of 112 species (Dias et al., 2020). Bulrushes had the lowest overall richness with 38 species and only 2–18 species per habitat island, while washouts harboured 42 species with 3–30 species per island (Dias et al., 2020). We obtained permission to work on livestock ranches directly from landowners or managers. No specific animal ethics approvals were required for this study, as birds were only observed in the field and were not captured or manipulated.

2.4 | Functional traits

We used six continuous traits measured from regional museum specimens that summarize functional information about avian body size and their feeding, walking and flying apparatuses: (i) body mass, (ii) length of the exposed culmen/length of the cranium, (iii) culmen curvature, (iv) toe span, (v) curvature of the claw of the middle toe and (vi) length of the closed wing (Dias et al., 2020). All length measurements were divided by the cubic root of body mass to account for allometric differences. Traits have a low correlation with each other ($r < 0.7$) and are not phylogenetically conserved (Dias et al., 2020). As such, we used the individual traits to calculate FD rather than first undertaking dimensionality reduction analyses.

The selected traits describe complementary aspects of avian functional diversity. Body mass correlates with metabolic rate, foraging behaviour, longevity and home range size (Luck et al., 2012). The morphology of the bill and feet is related to various aspects of foraging behaviour, such as the type of food consumed, food location and consumption (Botero-Delgadillo & Bayly, 2012; Luck et al., 2012). Wing morphology is linked to movement capacity and resource use. Longer wings relative to body size enable birds to disperse and migrate over long distances, linking resources more efficiently among isolated habitats (Botero-Delgadillo & Bayly, 2012; Claramunt et al., 2011).

2.5 | FD indices

We built a species-trait matrix including all species across the three datasets (i.e. a single 'global' trait space), using raw trait values, except for body mass which was log-transformed to correct for skewness, and a community matrix with the abundance of each species in each island (Tables S1.1–S1.6). The trait data were then centralized and normalized (i.e. *z*-scores). These six traits were used to build Gaussian kernel density *n*-dimensional hypervolumes for each island, based on Euclidean distances (Blonder et al., 2014, 2018; Mammola & Cardoso, 2020) with the 'kernel.build' function of the BAT R package version 2.9.2 (Cardoso et al., 2022) for R version 4.2.2 (R Core Team, 2023). We used consistent bandwidth values across all hypervolumes; these bandwidth values were calculated using the 'estimate_bandwidth' function from the hypervolume R package and the trait data for all species across our datasets (Ali et al., 2023; Blonder et al., 2018). The Gaussian method approximates trait values as clouds of stochastic points sampled from the set of observed trait values of the species in the community (Blonder et al., 2018). When abundance data are used, each observation is weighted by replicating it times the abundance in the estimation of the hypervolume. We used the 'kernel.alpha', 'kernel.dispersion' and 'kernel.evenness' functions of the BAT package to calculate indices of functional richness (FRic), functional divergence (FDiv) and functional regularity (FReg, which is sometimes termed functional evenness). All three indices were calculated using abundance data, and FRic was also calculated using presence–absence data. FRic is expressed as the total volume of the *n*-dimensional hypervolume (Cardoso et al., 2022; Mammola & Cardoso, 2020). FDiv was calculated with the 'kernel divergence' method and is expressed as the average distance between stochastic points within the hypervolume and the centroid of these points (Cardoso et al., 2022; Carmona et al., 2019). FReg describes the functional evenness of a community and is calculated as the overlap between the observed hypervolume and a theoretical hypervolume where traits and abundances are evenly distributed within the range of their values (Cardoso et al., 2022; Carmona et al., 2016, 2019). We built a correlation table for each island system to explore relationships between the three FDα indices, SR and abundance. As some authors have warned against using relatively large numbers of axes in hypervolume construction when sample size is limited (e.g. Blonder et al., 2014), we re-built the hypervolumes (with abundance data) using only three axes (re-calculating the bandwidth values using these three axes) and correlated the resultant three FDα indices with the equivalent versions from our main analyses. To generate the three axes, we performed a Principal Component Analysis using our full species-trait matrix, extracting the first three axes.

We used null models to calculate SES of the FDα indices. Our procedure involved randomizing the species in the trait matrix to avoid species having trait combinations that lack biological significance, such as breaking allometry rules. This method is analogous to the 'taxa.labels' method of the R package picante (Kembel et al., 2010). This randomized trait matrix was then used to calculate the three FDα indices. We repeated this procedure 999 times. The null model treats each island independently, and island species richness is fixed at the observed value. We estimated SES and associated *p*-values for each of the three FDα indices using the BAT function 'ses' to assess the significance of the deviation of observed values from the null expectations. Statistically significant ($p < 0.05$) positive FD.SES values indicate overdispersion, while clustering is indicated by statistically significant ($p < 0.05$) negative FD.SES values. Non-significant FD.SES values indicate random community assembly patterns. We reran the null models using the effect size (ES) approach (Matthews et al., 2023) and obtained consistent results (Figure S1.7). We only computed SES for abundance-weighted FRic, omitting presence–absence FRic due to their strong correlation, and because we also calculated abundance-weighted FDiv and FReg, thus ensuring comparability.

2.6 | Knowledge gaps I and II—FDAR modelling procedures

We modelled FDARs in arithmetic space by comparing the fit of 20 SAR models using the 'sar_average' function of the sars R package version 2.0.0 (Matthews et al., 2019) and an Information Theoretic approach (Burnham & Anderson, 2002). Models were fit in arithmetic space to enable clearer ecological interpretation, ensure comparability across indices and systems, and avoid artefacts introduced by log-transformations, which can alter model forms and obscure differences in functional diversity–area relationships (Tjørve, 2003, 2009; Triantis et al., 2012). In arithmetic space, models were assessed for normality via the Shapiro–Wilk test and for homoscedasticity of residuals via a Pearson's product–moment correlation between residuals and area ($\alpha = 0.05$ for both tests). Normality and homoscedasticity tests were not performed during the initial run of the 'sar_average' function for ease, but were conducted afterwards, only for the most plausible models (see below). The model selection was run separately for each of the three island systems and each of FRic, FDiv and FReg. Simple linear regression was used for the linear model, while the remaining models were fitted using nonlinear regression (Matthews et al., 2019). In the latter case, the selection of model starting parameter values was undertaken using a grid search method (we set the 'grid_start' argument to 'exhaustive' with 1000 sampling points). It should be noted that functionality in the sars R package places constraints on some models (to enable better fitting properties in most use cases) such that they are not able to provide good fits to negative relationships. As such, a small number of the 20 models are unlikely to provide good fits to the hypothesized FReg–area relationships. The observed shape of a model fit is determined using a sequential algorithm that identifies whether the fit is a straight line or, if not, classifies the observed shape as convex or sigmoidal based on analysis of the second derivative of the fit. We evaluated model performance using the second-order Akaike information criterion (AIC_c), selecting the model with the lowest AIC_c value as the most plausible (Burnham & Anderson, 2002). Models with ΔAIC_c (i.e., the relative difference in AIC_c values between each model and the most plausible model) <2 were considered to have similar empirical support. We used AIC_c weights ($wAIC_c$) to estimate the probability of each model being the best fit for the data among the set of models considered.

In the bulrush and washout datasets, the distribution of island area values is uneven, with a small number of relatively large habitat islands and many relatively small islands. To assess whether the individual larger islands have an undue influence on the model fits, we undertook a jackknife-type cross-validation procedure, testing the effect of the three largest islands. For a given dataset, we removed the largest island and re-ran the model fitting and comparison. We then re-instated this data point and removed the second largest island, and so on.

We further evaluated if the rate of change in diversity with increasing area differed among the three dimensions of FDα. We used the 'lin_pow' function from the sars R package to fit log–log power models for all our datasets and obtain comparable *z*-values (Tjørve, 2009).

2.7 | Knowledge gap III—Modelling FDAR.SES values and assessing the scaling of trait-based community assembly patterns

To determine whether there was any systematic change in FDα.SES values along the habitat island area gradient, given that strong FDARs often result from correlations between functional diversity and species richness (Dias et al., 2020; Matthews et al., 2023), for each island system separately we compared the fit of a null (intercept-only) model, a linear model and two piecewise breakpoint regression models, using the 'sar_threshold' function in the sars R package (Matthews & Rigal, 2021). Piecewise breakpoint regression models were used because dominant community assembly processes may vary across spatial scales (Gao & Wang, 2024), and these models have previously been shown to be useful for modelling how SES values scale with area (Matthews et al., 2020). We did not fit the set of 20 SAR models used above here as there are no theoretical reasons to expect convex or sigmoidal shaped relationships for SES–area relationships (Matthews et al., 2023). The breakpoint models comprised the one-threshold continuous model and the one-threshold zero slope model (where the first segment has a slope of zero). Within the 'sar_threshold' function, we set the 'interval' argument to 0.001 and the 'nisl' argument (the minimum number of islands to be contained within each segment, in the case of the breakpoint models) to five. Models were compared using AIC_c and, following Matthews et al. (2020, 2023), we fitted the models in semi-log space ($\log_{10}$). If the null model had the lowest AIC_c value or a ΔAIC_c value <2, we considered there to be no relationship between SES values and area.

3 | RESULTS

3.1 | Avian abundance and FD

Bird abundance was highest in washouts, followed by grasslands and bulrushes (Tables S1.8–S1.10). FRic values based on presence–absence data were higher than values associated with abundance-weighted data but showed the same trend, with the highest values in grasslands and the lowest in bulrushes. FDiv was similar in grasslands and washouts but slightly lower in bulrushes, while FReg was highest in bulrushes and lowest in washouts. In all island systems, strong positive correlations ($r \geq 0.7$) were observed between abundance, SR and the abundance-weighted and presence–absence FRic values (obtained from a correlation table; Table S1.11). FDiv and FReg exhibited strong negative correlations in grasslands and bulrushes ($r = -0.9$ and -0.8, respectively), but less so in washouts ($r = -0.5$).

For both FRic and FDiv, the FDα values generated using hypervolumes built with three trait axes were highly correlated with those used in our main analyses (Pearson's $r > 0.90$; Table S1.12). The correlations involving FReg were lower, which makes sense as this metric involves calculating and overlapping two hypervolumes, although only substantially so for washouts (grassland: $r = 0.84$; bulrush: $r = 0.69$; washout: $r = 0.27$).

3.2 | Knowledge gaps I and II—FDAR models

From the 20 candidate models, between 1 and 4 models were selected for each dimension of FDα per habitat island system based on the criteria of lowest AIC_c and $wAIC_c > 0.1$ (Table 1; Figure 1; complete results of the modelling procedures are detailed in Tables S1.13–S1.16). Presence–absence versus abundance-weighted FRic FDARs were best fit by the same model types and displayed similar patterns. No single model was included among the most plausible models best fitting FRic FDARs across the three island systems. FRic FDARs were convex-upwards in bulrushes, mostly sigmoidal in washouts, and both convex-upward and sigmoidal model fits were observed in grasslands. Non-asymptotic FDARs were found in bulrushes for both presence–absence and abundance-weighted FRic. In grasslands, abundance-weighted FRic FDARs were asymptotic, as they were for both presence–absence and abundance-weighted FRic in washouts. Of the most plausible models in bulrushes and washouts, presence–absence FRic FDAR models violated the assumption of homogeneity of variances, while abundance-weighted FRic models violated this assumption only in the bulrush system. Area explained most of the variation in all FRic analyses, with adjusted R^2 values of the most plausible models varying between 0.62 and 0.83.

The most plausible models best fitting FDiv and FReg FDARs also differed across our island systems. Only in grasslands was the most plausible FDiv FDAR model convex-upward and asymptotic. In the remaining island systems, FDiv FDAR model fits were non-asymptotic and mostly sigmoidal. FReg FDAR model fits were largely convex-downward and non-asymptotic, except in washouts, where they were sigmoidal or convex-upward in one instance. All the most plausible models best fitting FReg in bulrushes violated the assumption of homogeneity of variances. Adjusted R^2 values of the most plausible FDiv and FReg FDAR models were lower than for the FRic models, varying between 0.17 and 0.28 in the former and 0.11 and 0.43 in the latter.

Our jackknife cross-validation sensitivity test indicated that the selection of the best model (i.e., the model with the lowest AIC_c value) was relatively robust to the removal of individual larger islands (Table S1.17). In the 36 jackknife model comparisons (3 datasets × 4 FD indices × 3 individual data point removals), the original best model remained the best model in 30 cases and was only out of the top three in two cases.

The *z*-values of the log–log power model demonstrated that FRic (mean $z = 0.35$ for presence–absence and 0.29 for abundance-weighted) accumulated faster with increasing area than FDiv (mean $z = 0.04$; Table 2; Figure 2). FReg (mean $z = -0.17$) declined with area, in grasslands and bulrushes rather abruptly.

3.3 | Knowledge gap III—Modelling FDAR.SES values and assessing the scaling of trait-based community assembly patterns

Standardized effect sizes of FD indices showed no relationship with area, as intercept-only models were consistently the best fit or within 2 AIC_c units of the top model (Table 3; Figure 3). Across all islands in the three systems, most SES values for the three FDα indices were non-significant (59%–80% in grasslands, 79%–90% in bulrushes 73%–91% in washouts), indicating random trait-based community assembly (Figure 3). Overall, FRic.SES and FDiv.SES exhibited similar assembly patterns (i.e., most islands had non-significant SES values), though the use of FRic.SES resulted in relatively more islands with a significantly clustered pattern (31% of the total 110 islands vs. 24% for FDiv.SES). Overdispersion was detected only with FReg.SES, occurring in 9%–20% of islands across all three systems. Grasslands had the highest number of islands with a significantly clustered assembly pattern for both FRic.SES and FDiv.SES, while washouts showed the lowest occurrence of significant overdispersion for FReg.SES. FRic.SES and FDiv.SES clustering spanned the full area gradient in grasslands and washouts but was rarer in the smallest washouts. In bulrushes, clustering was detected mostly for mid-sized islands. FReg.SES overdispersion was limited to small and, particularly, mid-sized islands.

Most habitat islands with non-random assembly patterns (i.e., significant clustering or overdispersion) in one dimension also showed non-random patterns in others, but not always the same pattern (Figure S1.18). For example, islands displaying significant clustering with FRic.SES often showed this same pattern with FDiv.SES, while islands displaying significant overdispersion with FReg.SES often also displayed clustering with FRic.SES and FDiv.SES.

TABLE 1 Most plausible models describing multidimensional avian functional diversity–area relationships in three habitat island systems.

	$wAIC_c$	AIC_c	Shape	Asymptote	R^2	R^2 (adj)	*c*	*z*	*d*	*f*	*m*	Nor	Hom
Richness dimension													
Grassland system—presence–absence FRic													
Monod	0.12	598.68	U↑	Yes	0.68	0.66	0.02	-	1261.4	-	-	✓	✓
Grassland system—abundance-weighted FRic													
Logistic	0.12	588.71	S	Yes	0.66	0.64	0.91	66.03	915.16	-	-	✓	✓
Gompertz	0.11	588.79	S	Yes	0.66	0.64	0.01	50.73	925.55	-	-	✓	✓
Monod	0.11	588.87	U↑	Yes	0.64	0.63	0.02	-	1066.70	-	-	✓	✓
Bulrush system—presence–absence FRic													
Power	0.24	517.84	U↑	No	0.78	0.77	2513.90	0.33	-	-	-	✓	×
Extended power 1	0.12	519.32	U↑	No	0.78	0.77	3665.64	0.51	−0.04	-	-	✓	×
Power Rosenzweig	0.11	519.44	U↑	No	0.78	0.76	3001.80	0.42	-	93.87	-	✓	×
Persistence function 2	0.10	519.61	S	No	0.78	0.76	2700.80	0.35	0.00	-	-	✓	×
Bulrush system—abundance-weighted FRic													
Power	0.24	506.26	U↑	No	0.63	0.62	1334.20	0.25	-	-	-	✓	×
Washout system—presence–absence FRic													
Logistic	0.41	294.52	S	Yes	0.85	0.83	1.36	230.79	1500.40	-	-	✓	×
Gompertz	0.20	296.01	S	Yes	0.84	0.82	0.00	148.61	1522.90	-	-	✓	×
Washout system—abundance-weighted FRic													
Logistic	0.25	270.68	S	Yes	0.81	0.78	0.88	147.85	884.19	-	-	✓	✓
Gompertz	0.18	271.36	S	Yes	0.80	0.77	0.00	93.74	921.60	-	-	✓	✓
Asymptotic	0.12	272.16	U↑	Yes	0.80	0.76	760.14	0.00	1012.30	-	-	✓	✓
Divergence dimension													
Grassland system—FDiv													
Monod	0.16	−24.34	U↑	Yes	0.31	0.28	0.00	-	2.31	-	-	✓	✓
Bulrush system—FDiv													
Extended power 2	0.18	32.07	S	No	0.27	0.22	3.30	0.08	0.00	-	-	×	✓
Persistence function 2	0.17	32.23	S	No	0.27	0.21	3.34	0.09	0.00	-	-	×	✓
Power	0.10	33.27	U↑	No	0.21	0.17	2.92	0.06	-	-	-	✓	✓
Washout system—FDiv													
Extended power 1	0.26	11.27	S	No	0.29	0.17	20.03	1.13	−0.18	-	-	✓	✓
Linear	0.14	12.54	/	No	0.14	0.05	2.13	-	-		10.21	✓	✓
Persistence function 2	0.12	12.87	S	No	0.24	0.11	3.26	0.08	0.00	-	-	✓	✓

(Continues)

TABLE 1 (Continued)

	$wAIC_c$	AIC_c	Shape	Asymptote	R^2	R^2 (adj)	*c*	*z*	*d*	*f*	*m*	Nor	Hom
Regularity dimension													
Grassland system—FReg													
Power	0.31	−106.19	U↓	No	0.45	0.43	0.04	−0.41	-	-	-	✓	✓
Chapman Richards	0.17	−105.04	U↓	Yes	0.47	0.43	−0.55	28.32	0.12	-	-	✓	×
Extended power 1	0.17	−105.04	U↓	No	0.47	0.43	2.56	3.51	−0.42	-	-	✓	×
Power Rosenzweig	0.17	−104.94	U↓	No	0.46	0.43	0.01	−0.71	-	0.09	-	✓	×
Bulrush system—FReg													
Logarithmic	0.28	−12.78	U↓	No	0.23	0.19	−0.17	−0.07	-	-	-	✓	×
Power	0.24	−12.45	U↓	No	0.23	0.19	0.05	−0.27	-	-	-	✓	×
Washout system—FReg													
Persistence function 1	0.15	−35.84	S	No	0.23	0.11	13445000.00	2.46	1330.30	-	-	✓	✓
Negative exponential	0.14	−35.66	U↑	Yes	0.11	0.02	-	1891.30	0.16	-	-	×	×
Extended power 1	0.13	−35.56	S	No	0.22	0.10	0.00	−37.50	−0.16	-	-	✓	✓

Note: Models were selected based on the corrected Akaike's information criterion values (AIC_c) and weights ($wAIC_c$). Only models within <2 ΔAIC_c of the most plausible model and with $wAIC_c$ ≥0.1 are shown. Model shape (U: convex; /: linear; S: sigmoid; ↑: oriented upwards; ↓: oriented downwards), presence or absence of an asymptote, and values of the coefficient of determination (R^2; adjusted R^2) and of the fitted parameters *c*, *d*, *m*, and *z*, are given. The '✓' and '×' indicate satisfaction or violation, respectively, of the normality of the residuals (Nor) and the homogeneity of variances (Hom) assumptions. See Triantis et al. (2012) for the model functions and asymptote parameters.

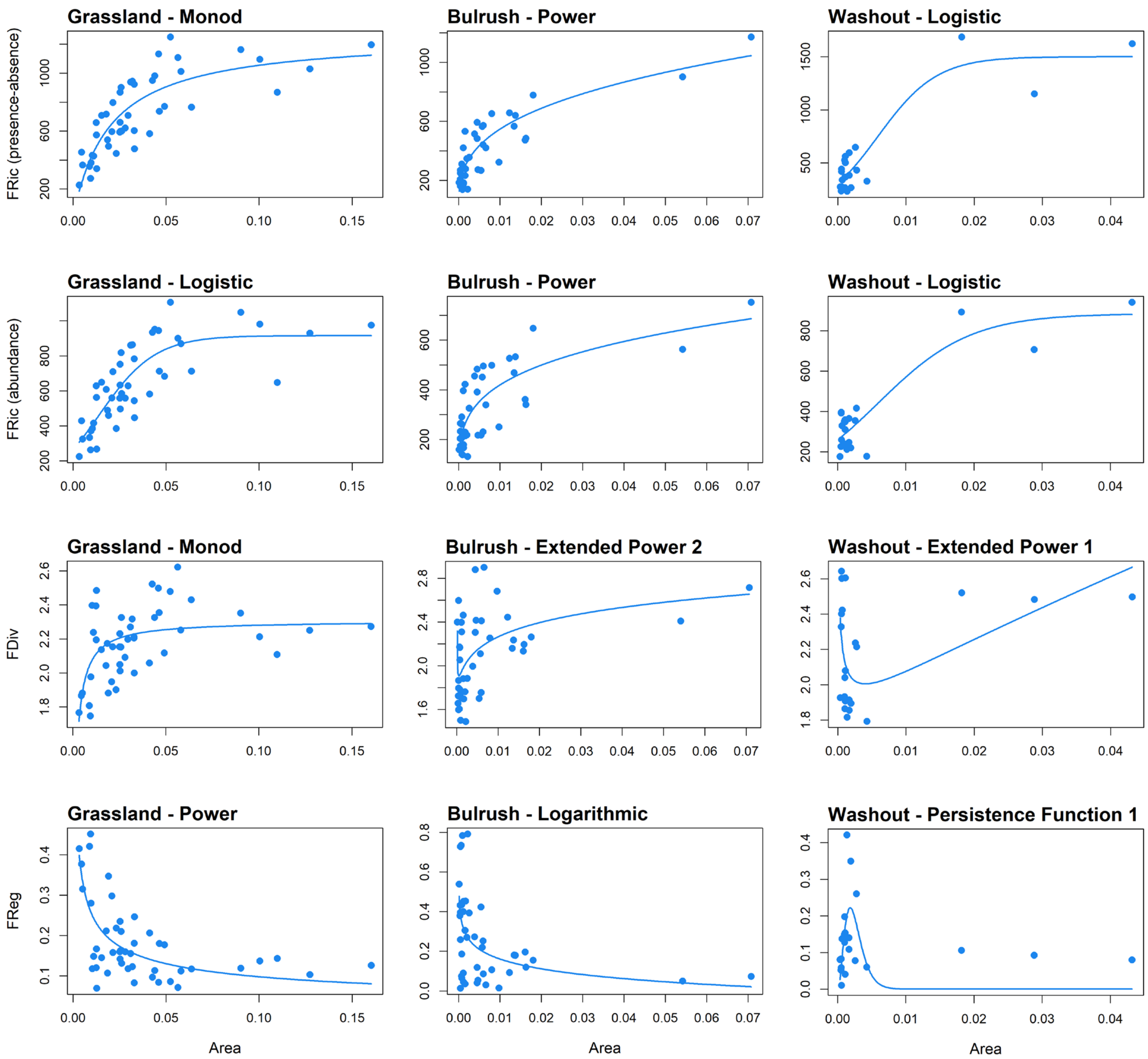

FIGURE 1 Functional richness– (FRic, both presence–absence based and abundance-weighted), divergence– (FDiv), and regularity– (FReg) area relationships in three habitat island systems. Only the most plausible model fit (i.e. the model with the lowest AIC$_c$ value; solid line) is shown in each case.

Some grassland and bulrush islands exhibited non-random patterns across all three dimensions.

4 | DISCUSSION

Previous FDAR studies have primarily focused on FRic, or, when addressing other FD dimensions, failed to explore a diverse range of model types (e.g., Dias et al., 2020; Karadimou et al., 2016; Matthews et al., 2023). Using an analytical framework that evaluated different FDAR models across multiple dimensions of FDα, we identified high variability in their type and shape, including asymptotic and sigmoidal patterns. Despite such variability, FRic and FDiv tended to increase with area, the former more rapidly, while FReg tended to decline. Our findings also showed that FRic FDARs were consistent across presence–absence and abundance-weighted data, reflecting the strong correlation between species richness and abundance. Controlling for species richness nullified the observed FDARs, confirming that species richness is the main driver of variation in functional diversity with area in habitat islands, as shown previously for presence-absence FRic (Dias et al., 2020; Matthews et al., 2023). The limited evidence of significant trait clustering and overdispersion suggests that stochastic processes dominate trait-based community assembly in our study systems. Our findings reinforce the

TABLE 2 *z*-values of log–log power models fitted to multidimensional functional diversity–area relationships in three habitat island systems.

	z-value (log–log)	z-value (arithmetic)	R^2(adj)	Nor	Hom
Richness dimension					
Grassland system—presence–absence FRic	0.40	0.34	0.68	×	✓
Grassland system—abundance-weighted FRic	0.37	0.31	0.64	✓	✓
Bulrush system—presence–absence FRic	0.31	0.33	0.67	✓	✓
Bulrush system—abundance-weighted FRic	0.24	0.25	0.56	✓	✓
Washout system—presence-absence FRic	0.35	0.39	0.64	✓	✓
Washout system—abundance-weighted FRic	0.26	0.31	0.50	✓	✓
Divergence dimension					
Grassland system—FDiv	0.06	0.06	0.28	✓	✓
Bulrush system—FDiv	0.05	0.06	0.18	✓	×
Washout system—FDiv	0.02	0.02	−0.02	✓	✓
Regularity dimension					
Grassland system—FReg	−0.32	−0.41	0.32	✓	✓
Bulrush system—FReg	−0.27	−0.27	0.02	×	✓
Washout system—FReg	0.07	0.01	−0.04	✓	✓

Note: *z*-values of power models fitted in arithmetic space and adjusted R^2 values of the log–log power model fits are also given. The '✓' and '×' indicate satisfaction or violation, respectively, of the normality of the residuals (Nor) and the homogeneity of variances (Hom) assumptions for the log–log power model fits.

importance of using a multidimensional FDα framework, which can uncover assembly patterns not detectable through single-dimension analyses.

4.1 | Knowledge gap I—Effect of species abundances on FRic FDARs

Using kernel density *n*-dimensional hypervolumes allowed us to compare presence-absence and abundance-weighted FRic FDARs. We found no major differences in the type and characteristics of models best fitting these relationships within island systems. However, presence–absence models had steeper slopes than abundance-weighted models, likely because the stochastic points in hypervolume-based trait space tend to cluster around the traits of abundant species, leaving unoccupied regions elsewhere and thereby reducing the expansion of FRic as area increases.

4.2 | Knowledge gap II—Comparing model shape and slope of FRic, FDiv and FReg FDARs

Contrary to our expectations, we found considerable variability in the type, shape, orientation and the presence (or absence) of an asymptote in models best fitting FDARs. While previous studies using presence–absence data, functional dendrograms and the same set of 20 candidate models have demonstrated that FRic FDARs were primarily characterized by non-asymptotic convex-upward models of the power and exponential families (Dias et al., 2020; Matthews et al., 2023), our results revealed a broader spectrum of relationship forms. Specifically, we identified asymptotic and sigmoidal relationships in some cases, which suggests that FDα either stabilizes beyond certain thresholds or exhibits inflection points. However, it should be noted that the best fit models in a small number of cases have forms that are difficult to explain ecologically (e.g., FDiv in washout; Figure 1), a common occurrence in island species–area relationship model comparison analyses (Triantis et al., 2012).

FRic FDARs consistently had higher R^2 values than those of FDiv and FReg, indicating that habitat size more strongly predicts the total volume of trait space (i.e. the cloud of stochastic points sampled from species-level trait observations) than the internal structure of that space, such as the distribution or evenness of those points (Ding et al., 2013; Ferrari et al., 2023; Karadimou et al., 2016). The faster accumulation of FRic with area suggests that very small islands may fail to capture the full range of functional traits in a given system (Mammola et al., 2021; Matthews et al., 2023; Mazel & Thuiller, 2021; Mouchet et al., 2010). The decline in FReg with increasing area has been associated with the presence of more rare species and the higher abundances of common species in larger islands, which tend to expand the overall trait space but lead to a more uneven spread

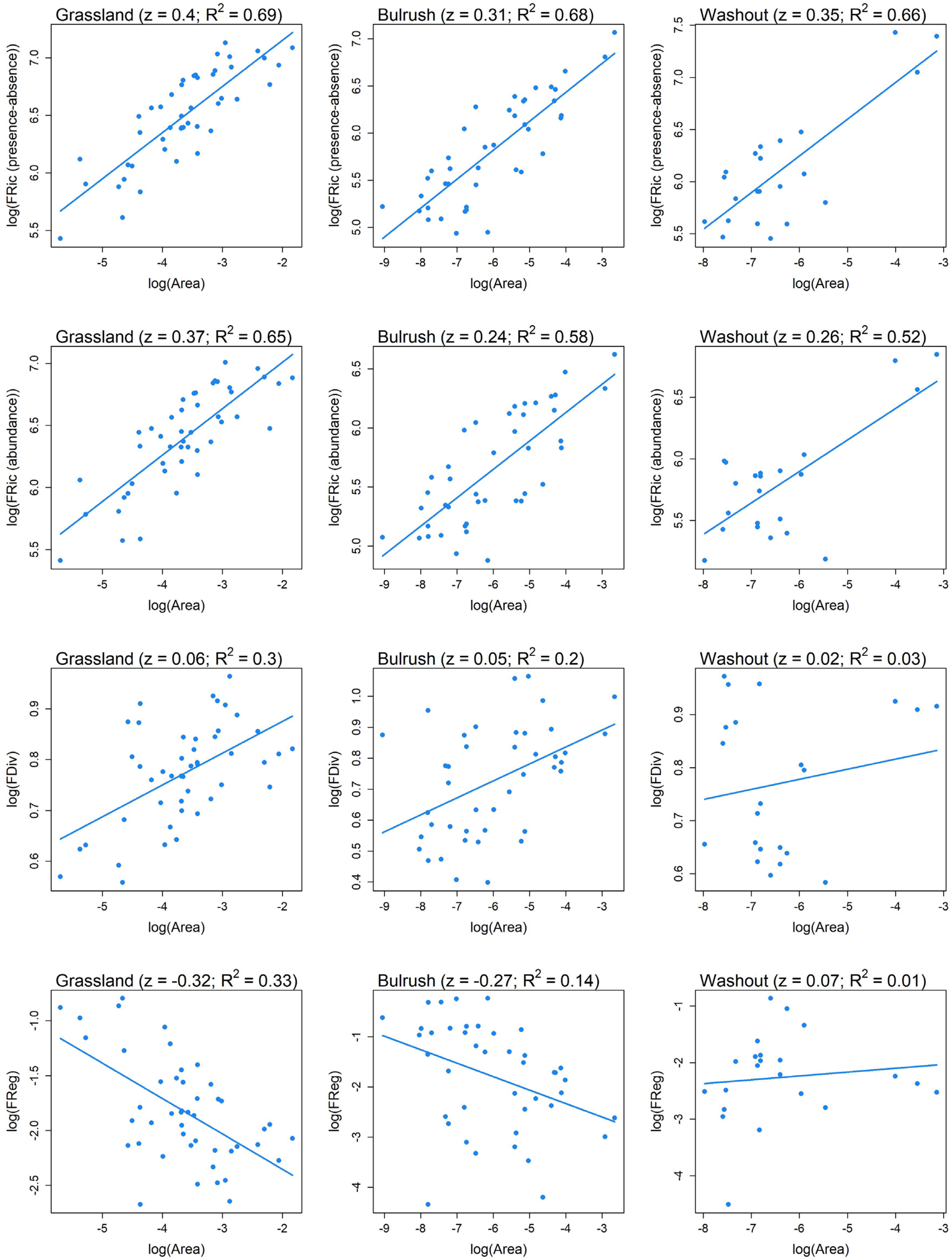

FIGURE 2 Functional diversity–area relationships fitted using a log–log transformation. The fit of a linear model (i.e. the log–log power model; solid line) is shown, with the associated *z*-value and R^2 value also presented. Note these are the standard R^2 values and thus differ slightly from the adjusted R^2 values provided in Table 2.

TABLE 3 Summary of the fit of piecewise, linear and intercept-only models of the relationship between island area and the standardized effect sizes of multidimensional avian functional diversity in three habitat island systems.

	AIC_c	R^2	Threshold 1	Segment 1	Segment 2
Richness dimension					
Grassland system—abundance-weighted FRic.SES					
Intercept-only	157.70	0.00	-	-	-
Linear	159.15	0.02	-	-	-
ZslopeOne	159.82	0.05	−1.13	41	5
ContOne	162.35	0.05	−1.13	41	5
Bulrush system—abundance-weighted FRic.SES					
Intercept-only	135.25	0.00	-	-	-
Linear	137.57	0.00	-	-	-
ZslopeOne	138.98	0.02	−1.79	37	5
ContOne	140.53	0.05	−2.67	22	20
Washout system—abundance-weighted FRic.SES					
Intercept-only	79.88	0.00	-	-	-
Linear	81.05	0.07	-	-	-
ZslopeOne	84.29	0.06	−3.25	5	17
ContOne	84.51	0.18	−2.90	12	10
Divergence dimension					
Grassland system—FDiv.SES					
ZslopeOne	146.88	0.11	−1.20	41	5
Intercept-only	147.35	0.00	-	-	-
Linear	147.74	0.04	-	-	-
ContOne	149.40	0.11	−1.20	41	5
Bulrush system—FDiv.SES					
Intercept-only	124.54	0.00	-	-	-
Linear	126.69	0.00	-	-	-
ZslopeOne	128.38	0.02	−1.79	37	5
ContOne	128.62	0.08	−3.34	6	36
Washout system—FDiv.SES					
ContOne	59.24	0.39	−2.91	12	10
Linear	59.84	0.15	-	-	-
Intercept-only	60.84	0.00	-	-	-
ZslopeOne	63.11	0.15	−3.25	5	17
Regularity dimension					
Grassland system—FReg.SES					
Intercept-only	171.16	0.00	-	-	-
Linear	172.16	0.03	-	-	-
ZslopeOne	174.94	0.02	−1.68	15	31
ContOne	175.46	0.06	−1.20	40	6
Bulrush system—FReg.SES					
Intercept-only	152.14	0.00	-	-	-
Linear	154.16	0.01	-	-	-
ZslopeOne	154.35	0.06	−1.79	37	5
ContOne	156.85	0.06	−1.79	37	5

TABLE 3 (Continued)

	AIC_c	R^2	Threshold 1	Segment 1	Segment 2
Washout system—FReg.SES					
ContOne	64.70	0.40	−2.87	13	9
Intercept-only	66.69	0.00	-	-	-
Linear	68.78	0.03	-	-	-
ZslopeOne	71.94	0.02	−3.25	5	17

Note: Models are ranked using the corrected Akaike's information criterion (AIC_c). 'ZslopeOne' is a left-horizontal model (i.e., the first slope is fixed at zero) with a single threshold, while 'ContOne' is a continuous model (i.e., both slopes can vary) with a single threshold. The models were fitted in semi-log space. Values of the coefficient of determination (R^2), the threshold values and the number of data points within each segment are given. Threshold 1 is the $\log_{10}$ threshold value, and Segment 1 and Segment 2 provide the number of data points within each segment.

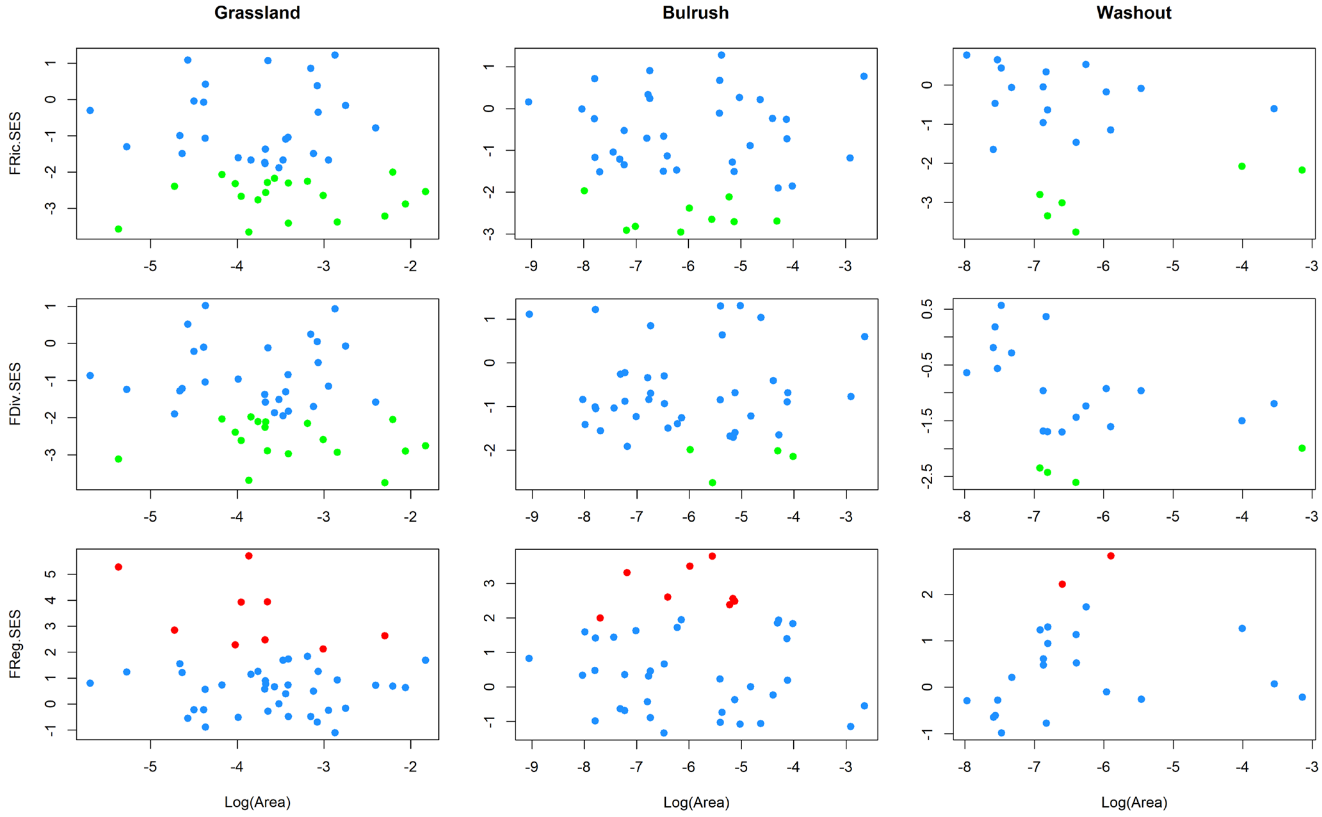

FIGURE 3 Relationships between standardized effect sizes (SES) of abundance-weighted FRic, FDiv and FReg and $\log_{10}$(area) in three habitat island systems. In all cases, the intercept-only model (not shown) was more, or as equally, plausible as the other candidate models. Red circles indicate islands with significantly more functional diversity than expected based on a null model (overdispersion), green circles indicate significantly less functional diversity than expected (clustering), and blue circles indicate functional diversity not different from expected (random assembly), given the regional species pool.

of species and individuals within trait space (Ding et al., 2013; Ferrari et al., 2023; Karadimou et al., 2016). This suggests that larger natural habitat islands may be less resilient to environmental change, as low functional redundancy in some regions of trait space may constrain the capacity of the system to respond effectively to disturbance (Karadimou et al., 2016; Mazel & Thuiller, 2021). The steeper FDAR slopes observed in the grassland system, where bird and habitat diversity are higher and the matrix is more permeable, may signal greater functional sensitivity to area reduction compared to the other systems. While limited sample size precludes comparisons, this pattern suggests that in more homogeneous and isolated habitat island systems (such as the bulrush and washout systems here), a few species adapted to the prevailing habitat conditions may occur across the entire island size gradient and maintain key functions despite area loss (Bastazini et al., 2019; González-del-Pliego et al., 2024; Henderson et al., 2020). Nonetheless, we acknowledge the debate over applying species–area relationships backwards to estimate diversity loss (Fattorini & Borges, 2012; He & Hubbell, 2013) and recognize that similar concerns likely extend to FDARs.

Large islands lacked the combination of relatively low FRic and FDiv with high FReg, while small and mid-sized islands exhibited greater variability in FDiv and FReg. This pattern is consistent with expectations, as low FRic and FDiv would indicate less and underutilized functional space, which is unlikely on large islands with greater resource availability (Ferrari et al., 2023; Mammola et al., 2021; Mouchet et al., 2010). In contrast, relatively high FDiv on some small and mid-sized islands may reflect the presence of a few abundant, functionally distinct species that partition limited resources more efficiently (Matthews et al., 2023; Mouchet et al., 2010). Why this only occurs on certain small and mid-sized islands is unknown. The variable FReg values observed in small islands likely reflect differences in species abundance and trait distributions, where some island assemblages comprise species with evenly spaced traits, possibly due to limiting similarity, while others are dominated by a few distinct species, leading to trait clustering (Ferrari et al., 2023; Karadimou et al., 2016; Mouchet et al., 2010). These patterns suggest that small and mid-sized islands may contribute to functional diversity in ways not captured by species richness alone, supporting the relevance of FDARs for identifying conservation value across the full range of island sizes (Dias et al., 2020). However, we acknowledge the need for caution in this interpretation given the potential influence of transient functionally distinct species that can disproportionately influence FDα indices (Basile, 2022), particularly on small and mid-sized habitat islands.

4.3 | Knowledge gap III—SES.FDAR models and the scaling of trait-based community assembly patterns

As expected, abundance-weighted SES.FRic, SES.FDiv, and SES.FReg showed no discernible relationship with island area, confirming that the scaling of unstandardized FDα indices with habitat island area is primarily due to increasing SR rather than systematic shifts in dominant community assembly processes (Dias et al., 2020; Ding et al., 2013; Matthews et al., 2023). Irrespective of the dimension investigated, random FDα values (i.e., FDα values not significantly different than expected based on our null model) dominated across systems. This finding supports previous studies arguing that neutral dynamics are likely the primary drivers of community assembly in habitat islands (Dias et al., 2020; MacArthur & Wilson, 1967; Matthews et al., 2023). However, these results could also be generated through a combination of different processes (e.g. habitat filtering and competition) acting simultaneously and effectively cancelling each other out.

Significant clustering (FDα values significantly lower than expected) was observed for FRic and FReg along the entire grassland area gradient but was absent on the smallest bulrush and washout, and largest bulrush, islands. While mostly non-significant, SES.FRic and SES.FDiv values were usually negative, indicating a weak tendency for clustering, consistent with other island community assembly research (Dias et al., 2020; Matthews et al., 2023; Si et al., 2022). Trait clustering is often associated with environmental filtering, a process that is theorized to act more strongly on islands with low habitat diversity, which typically are small (Dias et al., 2020; Ding et al., 2013; Matthews et al., 2023), but it may also be influenced by processes such as competition, which is also theorized to be stronger in relatively smaller habitat islands (Mayfield & Levine, 2010; Mouchet et al., 2010; Villéger et al., 2008).

Our results further emphasize the rarity of trait overdispersion (FDα values significantly higher than expected) in habitat islands (Dias et al., 2020; Gao & Wang, 2024; Matthews et al., 2023). Significant trait overdispersion was only detected when using FReg, a metric theoretically sensitive to competition effects at small scales (Mazel & Thuiller, 2021; but see Mouchet et al., 2010; Villéger et al., 2008 for discussion on its sensitivity to habitat filtering). Significant trait overdispersion was absent from the smallest and largest islands, particularly in bulrushes and washouts. Mid-sized islands may be more prone to trait overdispersion as they provide more niche space than smaller islands but remain limited compared to larger ones, potentially intensifying interspecific competition. This may result in the presence of multiple guilds, each containing a few species due to intensified interspecific competition, leading to functional overdispersion (Matthews et al., 2023).

Interestingly, some islands showed contrasting patterns across FDα dimensions, with significant clustering in one index and significant overdispersion in another. Rather than indicating a single dominant process, such divergence may reflect the operation of different filters acting on different aspects of trait structure (Mazel & Thuiller, 2021; Mouchet et al., 2010; Villéger et al., 2008). Nonetheless, interpretations of SES.FDiv and SES.FReg should be undertaken with caution given that the effects of richness correction on these dimensions are less understood.

5 | CONCLUSION

Our findings challenge traditional approaches to FDAR research by demonstrating the value of integrating multidimensional FDα in a unified analytical framework. This approach not only revealed variability in FDARs across FDα dimensions but also highlighted the potential influence of both within-island and between-island characteristics in shaping this variability. We encourage future FDAR research to systematically assess the relationships between species richness, abundance, and FDα metrics prior to model fitting to better understand the influence of taxonomic structure on functional diversity and to strengthen result interpretation. The complementary use of FRic, FDiv and FReg is essential to disentangle dominant community assembly processes and identify priority patches for conservation. Expanding this framework to other insular systems and exploring mechanisms such as environmental filtering and competition on community assembly at finer scales will enhance the generalizability of our findings. Simulation-based studies could also provide deeper insights into the occurrence of both trait clustering and overdispersion within habitat islands. Ultimately, a multidimensional perspective on FDARs is vital to advancing our understanding of community assembly and guiding conservation strategies in patchy environments.

AUTHOR CONTRIBUTIONS

Rafael Antunes Dias, Vinicius Augusto Galvão Bastazini and Thomas J. Matthews conceived the ideas and designed the methodology; Rafael Antunes Dias, Andros T. Gianuca and Vinicius Augusto Galvão Bastazini collected the data; Rafael Antunes Dias and Thomas J. Matthews analysed the data; Rafael Antunes Dias led the writing of the manuscript. All authors contributed critically to the drafts and gave final approval for publication.

ACKNOWLEDGEMENTS

Pedro Cardoso kindly provided advice regarding the hypervolume metrics. Alejandro Martínez García, Gabriel Nakamura, and Stefano Mammola assisted with the code used to calculate standardized effect sizes. Felipe C. Bonow and Maycon S. S. Gonçalves helped with fieldwork. Fieldwork was supported by the now-defunct Environmental Assessment Program of Universidade Católica de Pelotas, Brazil.

CONFLICT OF INTEREST STATEMENT

Vinicius Augusto Galvão Bastazini is an Associate Editor of *Functional Ecology*, but took no part in the peer review or decision-making processes for this paper. The remaining authors have no conflicts of interest.

DATA AVAILABILITY STATEMENT

Data are available from the Zenodo repository: https://doi.org/10.5281/zenodo.16901063 (Dias, 2025). The code used to reproduce the analyses is available on GitHub: https://github.com/bastazini/FDARs.

STATEMENT ON INCLUSION

This study was primarily conceived and conducted by researchers based in Brazil, the country where the research was carried out, reflecting local leadership and contributing to capacity building in the region.

ORCID

Rafael Antunes Dias https://orcid.org/0000-0001-7203-2093
Vinicius Augusto Galvão Bastazini https://orcid.org/0000-0001-5270-0621
Andros T. Gianuca https://orcid.org/0000-0001-9639-3846
Thomas J. Matthews https://orcid.org/0000-0002-7624-244X

REFERENCES

Ali, J. R., Blonder, B. W., Pigot, A. L., & Tobias, J. A. (2023). Bird extinctions threaten to cause disproportionate reductions of functional diversity and uniqueness. *Functional Ecology*, *37*, 162–175. https://doi.org/10.1111/1365-2435.14201

Basile, M. (2022). Rare species disproportionally contribute to functional diversity in managed forests. *Scientific Reports*, *12*, 5897. https://doi.org/10.1038/s41598-022-09624-9

Bastazini, V. A., Debastiani, V. J., Azambuja, B. O., Guimarães, P. R., & Pillar, V. D. (2019). Loss of generalist plant species and functional diversity decreases the robustness of a seed dispersal network. *Environmental Conservation*, *46*(1), 52–58. https://doi.org/10.1017/S0376892918000334

Blonder, B., Lamanna, C., Violle, C., & Enquist, B. J. (2014). The n-dimensional hypervolume. *Global Ecology and Biogeography*, *23*, 595–609. https://doi.org/10.1111/geb.12146

Blonder, B., Morrow, C. B., Maitner, B., Harris, D. J., Lamanna, C., Violle, C., Enquist, B. J., & Kerkhoff, A. J. (2018). New approaches for delineating n-dimensional hypervolumes. *Methods in Ecology and Evolution*, *9*, 305–319. https://doi.org/10.1111/2041-210X.12865

Botero-Delgadillo, E., & Bayly, N. J. (2012). Does morphology predict behavior? Correspondence between behavioral and morphometric data in a Tyrant-flycatcher (Tyrannidae) assemblage in the Santa Marta Mountains, Colombia. *Journal of Field Ornithology*, *83*, 329–342. https://doi.org/10.1111/j.1557-9263.2012.00383.x

Burnham, K. P., & Anderson, D. R. (2002). *Model selection and multimodel inference: A practical information-theoretic approach*. Springer-Verlag.

Cadotte, M., Albert, C. H., & Walker, S. C. (2013). The ecology of differences: Assessing community assembly with trait and evolutionary distances. *Ecology Letters*, *16*, 1234–1244. https://doi.org/10.1111/ele.12161

Cardoso, P., Mammola, S., Rigal, F., & Carvalho, J. (2022). *BAT: Biodiversity assessment tools*. R package version 2.9.2. https://CRAN.R-project.org/package=BAT

Carmona, C. P., de Bello, F., Mason, N. W. H., & Lepš, J. (2016). Traits without borders: Integrating functional diversity across scales. *Trends in Ecology & Evolution*, *31*, 382–394. https://doi.org/10.1016/J.TREE.2016.02.003

Carmona, C. P., de Bello, F., Mason, N. W. H., & Lepš, J. (2019). Trait probability density (TPD): Measuring functional diversity across scales based on TPD with R. *Ecology*, *100*, e02876. https://doi.org/10.1002/ecy.2876

Chase, J. M., Gooriah, L., May, F., Ryberg, W. A., Schuler, M. S., Craven, D., & Knight, T. M. (2019). A framework for disentangling ecological mechanisms underlying the island species–area relationship. *Frontiers of Biogeography*, *11*(1), e40844. https://doi.org/10.21425/F5FBG40844

Claramunt, S., Derryberry, E. P., Remsen, J. V., Jr., & Brumfield, R. T. (2011). High dispersal ability inhibits speciation in a continental radiation of passerine birds. *Proceedings of the Royal Society B: Biological Sciences*, *279*, 1567–1574. https://doi.org/10.1098/rspb.2011.1922

Dias, R. (2025). The spatial scaling of multiple dimensions of functional diversity in habitat islands [Data set]. Functional Ecology (1.0.0). *Zenodo*. https://doi.org/10.5281/zenodo.16901063

Dias, R. A., Bastazini, V. A. G., Knopp, B. D. C., Bonow, F. C., Gonçalves, M. S. S., & Gianuca, A. T. (2020). Species richness and patterns of overdispersion, clustering and randomness shape phylogenetic and functional diversity–area relationships in habitat islands. *Journal of Biogeography*, *47*, 1638–1648.

Ding, Z., Feeley, K. J., Wang, Y., Pakeman, R. J., & Ding, P. (2013). Patterns of bird functional diversity on land-bridge island fragments. *Journal of Animal Ecology*, *82*, 781–790. https://doi.org/10.1111/1365-2656.12046

Fattorini, S., & Borges, P. A. V. (2012). Species–area relationships underestimate extinction rates. *Acta Oecologica*, *40*, 27–30. https://doi.org/10.1016/j.actao.2012.02.006

Ferrari, D. S., Floeter, S. R., Leprieur, F., & Quimbayo, J. P. (2023). A trait-based approach to marine island biogeography. *Journal of Biogeography*, *50*, 528–538. https://doi.org/10.1111/jbi.14549

Gao, D., & Wang, Y. (2024). Non-linear thresholds in the effect of area on three dimensions of diversity of herpetofauna in the West Indies. *Journal of Biogeography*, *51*, 439–453. https://doi.org/10.1111/jbi.14765

González-del-Pliego, P., Galiana, N., González-Trujillo, J. D., Mestre, F., Araújo, M. B., & Bastazini, V. A. G. (2024). Are threatened species important for glueing interaction networks together? *Perspectives in Ecology and Conservation*, *22*(4), 342–347. https://doi.org/10.1016/j.pecon.2024.11.003

He, F., & Hubbell, S. (2013). Estimating extinction from species–area relationships: Why the numbers do not add up. *Ecology*, *94*, 1905–1912. https://doi.org/10.1890/12-1795.1

Henderson, C. J., Gilby, B. L., Schlacher, T. A., Connolly, R. M., Sheaves, M., Maxwell, P. S., Flint, N., Borland, H. P., Martin, T. S. H., & Olds, A. D. (2020). Low redundancy and complementarity shape ecosystem functioning in a low-diversity ecosystem. *The Journal of Animal Ecology*, *89*, 784–794. https://doi.org/10.1111/1365-2656.13148

Karadimou, E. K., Kallimanis, A. S., Tsiripidis, I., & Dimopoulos, P. (2016). Functional diversity exhibits a diverse relationship with area, even a decreasing one. *Scientific Reports*, *6*, 35420. https://doi.org/10.1038/srep35420

Kembel, S. W., Cowan, P. D., Helmus, M. R., Cornwell, W. K., Morlon, H., Ackerly, D. D., Blomberg, S. P., & Webb, C. O. (2010). Picante: R tools for integrating phylogenies and ecology. *Bioinformatics*, *26*, 1463–1464. https://doi.org/10.1093/bioinformatics/btq166

Lomolino, M. V. (2000). Ecology's most general, yet protean pattern: The species–area relationship. *Journal of Biogeography*, *27*, 17–26. https://doi.org/10.1046/j.1365-2699.2000.00377.x

Luck, G. W., Lavorel, S., McIntyre, S., & Lumb, K. (2012). Improving the application of vertebrate trait-based frameworks to the study of ecosystem services. *Journal of Animal Ecology*, *81*, 1065–1076. https://doi.org/10.1111/j.1365-2656.2012.01974.x

MacArthur, R. H., & Wilson, E. O. (1967). *The theory of island biogeography*. Princeton University Press.

Mammola, S., & Cardoso, P. (2020). Functional diversity metrics using kernel density *n*-dimensional hypervolumes. *Methods in Ecology and Evolution*, *11*, 986–995. https://doi.org/10.1111/2041-210X.13424

Mammola, S., Carmona, C. P., Guillerme, T., & Cardoso, P. (2021). Concepts and applications in functional diversity. *Functional Ecology*, *35*, 1869–1885. https://doi.org/10.1111/1365-2435.13882

Matthews, T. J. (2021). On the biogeography of habitat islands: The importance of matrix effects, noncore species, and source-sink dynamics. *The Quarterly Review of Biology*, *96*, 73–104.

Matthews, T. J., & Rigal, F. (2021). Thresholds and the species–area relationship: A set of functions for fitting, evaluating and plotting a range of commonly used piecewise models in R. *Frontiers of Biogeography*, *13*, e49404. https://doi.org/10.21425/F5FBG49404

Matthews, T. J., Rigal, F., Kougioumoutzis, K., Trigas, P., & Triantis, K. A. (2020). Unravelling the small-island effect through phylogenetic community ecology. *Journal of Biogeography*, *47*, 2341–2352. https://doi.org/10.1111/jbi.13940

Matthews, T. J., Triantis, K. A., Whittaker, R. J., & Guilhaumon, F. (2019). sars: An R package for fitting, evaluating and comparing species–area relationship models. *Ecography*, *42*(8), 1446–1455. https://doi.org/10.1111/ecog.04271

Matthews, T. J., Wayman, J. P., Whittaker, R. J., Cardoso, P., Hume, J. P., Sayol, F., Proios, K., Martin, T. E., Baiser, B., Borges, P. A. V., Kubota, Y., dos Anjos, L., Tobias, J. A., Soares, F. C., Si, X., Ding, P., Mendenhall, C. D., Sin, Y. C. K., Rheindt, F. E., … Rigal, F. (2023). A global analysis of avian island diversity–area relationships in the Anthropocene. *Ecology Letters*, *26*, 965–982. https://doi.org/10.1111/ele.14203

Mayfield, M. M., & Levine, J. M. (2010). Opposing effects of competitive exclusion on the phylogenetic structure of communities. *Ecology Letters*, *13*, 1085–1093. https://doi.org/10.1111/j.1461-0248.2010.01509.x

Mazel, F., & Thuiller, W. (2021). Functional and phylogenetic diversity–area relationships. In T. J. Matthews, K. A. Triantis, & R. J. Whittaker (Eds.), *The species–area relationship: Theory and application* (pp. 107–132). Cambridge University Press.

Mouchet, M. A., Villéger, S., Mason, N. W. H., & Mouillot, D. (2010). Functional diversity measures: An overview of their redundancy and their ability to discriminate community assembly rules. *Functional Ecology*, *24*, 867–876. https://doi.org/10.1111/j.1365-2435.2010.01695.x

Palacio, F. X., Callaghan, C. T., Cardoso, P., Hudgins, E. J., Jarzyna, M. A., Ottaviani, G., Riva, F., Graco-Roza, C., Shirey, V., & Mammola, S. (2022). A protocol for reproducible functional diversity analyses. *Ecography*, *2022*, e06287. https://doi.org/10.1111/ecog.06287

Pavoine, S., & Bonsall, M. B. (2011). Measuring biodiversity to explain community assembly: A unified approach. *Biological Reviews*, *86*, 792–812. https://doi.org/10.1111/j.1469-185X.2010.00171.x

R Core Team. (2023). *R: A language and environment for statistical computing*. R Foundation for Statistical Computing. https://www.r-project.org

Si, X., Cadotte, M. W., Davies, T. J., Antonelli, A., Ding, P., Svenning, J.-C., & Faurby, S. (2022). Phylogenetic and functional clustering illustrate the roles of adaptive radiation and dispersal filtering in jointly shaping late-Quaternary mammal assemblages on oceanic islands. *Ecology Letters*, *25*, 1250–1262. https://doi.org/10.1111/ele.13997

Smith, A. B., Sandel, B., Kraft, N. J., & Carey, S. (2013). Characterizing scale-dependent community assembly using the functional-diversity–area relationship. *Ecology*, *94*, 2392–2402. https://doi.org/10.1890/12-2109.1

Tjørve, E. (2003). Shapes and functions of species–area curves: a review of possible models. *Journal of Biogeography*, *30*, 827–835. https://doi.org/10.1046/j.1365-2699.2003.00877.x

Tjørve, E. (2009). Shapes and functions of species–area curves (II): A review of new models and parameterizations. *Journal of Biogeography*, *36*, 1435–1445. https://doi.org/10.1111/j.1365-2699.2009.02101.x

Tjørve, E., Kunin, W. E., Polce, C., & Tjørve, K. M. C. (2008). Species-area relationship: Separating the effects of species abundance and spatial distribution. *Journal of Ecology*, *96*, 1141–1151.

Tobias, J. A., Sheard, C., Pigot, A. L., Devenish, A. J. M., Yang, J., Sayol, F., Neate-Clegg, M. H. C., Alioravainen, N., Weeks, T. L., Barber, R. A., Walkden, P. A., MacGregor, H. E. A., Jones, S. E. I., Vincent, C., Phillips, A. G., Marples, N. M., Montaño-Centellas, F. A., Leandro-Silva, V., Claramunt, S., … Schleuning, M. (2022). AVONET: Morphological, ecological and geographical data for all birds. *Ecology Letters*, *25*, 581–597. https://doi.org/10.1111/ele.13898

Triantis, K. A., Guilhaumon, F., & Whittaker, R. J. (2012). The island species–area relationship: Biology and statistics. *Journal of Biogeography*, *39*, 215–231. https://doi.org/10.1111/j.1365-2699.2011.02652.x

Villéger, S., Mason, N. W. H., & Mouillot, D. (2008). New multidimensional functional diversity indices for a multifaceted framework in functional ecology. *Ecology*, *89*, 2290–2301. https://doi.org/10.1890/07-1206.1

Weiher, E., & Keddy, P. (1995). Assembly rules, null models, and trait dispersion: New questions from old patterns. *Oikos*, *74*, 159–164. https://doi.org/10.2307/3545686

SUPPORTING INFORMATION

Additional supporting information can be found online in the Supporting Information section at the end of this article.

Data S1. Table S1.1. Mean functional trait values for each species in grasslands. Length measurements were divided by the cubic root of body mass.

Table S1.2. Mean functional trait values for each species in bulrushes. Length measurements were divided by the cubic root of body mass.

Table S1.3. Mean functional trait values for each species in washouts. Length measurements were divided by the cubic root of body mass.

Table S1.4. Bird abundance per grassland habitat island.

Table S1.5. Bird abundance per bulrush habitat island.

Table S1.6. Bird abundance per washout habitat island.

Table S1.7. Pearson correlations between standardized effect sizes (SES) and effect sizes (ES) of functional richness (FRic), functional divergence (FDiv) and functional regularity.

Table S1.8. Dataset for grassland habitat islands.

Table S1.9. Dataset for bulrush habitat islands.

Table S1.10. Dataset for washout habitat islands.

Table S1.11. Pearson correlations between diversity indices.

Table S1.12. Pearson correlations between functional diversity indices based on multiple axes and those based on three axes.

Table S1.13. Complete results of the model selection procedure for presence–absence-based Fric.

Table S1.14. Complete results of the model selection procedure for abundance-weighted FRic.

Table S1.15. Complete results of the model selection procedure for FDiv.

Table S1.16. Complete results of the model selection procedure for FReg.

Table S1.17. Results of the jackknife-type cross-validation exercise.

Figure S1.18. Upset plots showing the number of habitat islands exhibiting trait clustering (identified with FRic and FDiv) and overdispersion (identified with FReg) in three habitat island systems.

How to cite this article: Dias, R. A., Bastazini, V. A. G., Gianuca, A. T., & Matthews, T. J. (2025). The spatial scaling of multiple dimensions of functional diversity in habitat islands. *Functional Ecology*, *00*, 1–17. https://doi.org/10.1111/1365-2435.70158